Biochemical and Biophysical Research Communications 431 (2013) 239–245

Contents lists available at SciVerse ScienceDirect

Biochemical and Biophysical Research Communications

journal homepage: www.elsevier.com/locate/ybbrc

Role of Na^+–H^+ exchange in the modulation of L-type Ca^{2+} current during fluid pressure in rat ventricular myocytes

Joon-Chul Kim, Sun-Hee Woo *

Laboratory of Physiology, College of Pharmacy, Chungnam National University, 220 Gungdong, Daejeon 305-764, South Korea

ARTICLE INFO

Article history:
Received 27 December 2012
Available online 9 January 2013

Keywords:
Na^+–H^+ exchange
Fluid pressure
L-type Ca^{2+} current
HOE642
Ventricular myocytes

ABSTRACT

Application of fluid pressure (FP) using pressurized fluid flow suppresses the L-type Ca^{2+} current through both enhancement of Ca^{2+} release and intracellular acidosis in ventricular myocytes. As FP-induced intracellular acidosis is more severe during the inhibition of Na^+–H^+ exchange (NHE), we examined the possible role of NHE in the regulation of I_{Ca} during FP exposure using HOE642 (cariporide), a specific NHE inhibitor. A flow of pressurized (~16 dyn/cm^2) fluid was applied onto single rat ventricular myocytes, and the I_{Ca} was monitored using a whole-cell patch-clamp under HEPES-buffered conditions. In cells pre-exposed to FP, additional treatment with HOE642 dose-dependently suppressed the I_{Ca} (IC_{50} = 0.97 ± 0.12 μM) without altering current–voltage relationships and inactivation time constants. In contrast, the I_{Ca} in control cells was not altered by HOE642. The HOE642 induced a left shift in the steady-state inactivation curve. The suppressive effect of HOE642 on the I_{Ca} under FP was not altered by intracellular high Ca^{2+} buffering. Replacement of external Cl^- with aspartate to inhibit the Cl^--dependent acid loader eliminated the inhibitory effect of HOE642 on I_{Ca}. These results suggest that NHE may attenuate FP-induced I_{Ca} suppression by preventing intracellular H^+ accumulation in rat ventricular myocytes and that NHE activity may not be involved in the Ca^{2+}-dependent inhibition of the I_{Ca} during FP exposure.

1. Introduction

Activation of cardiac L-type Ca^{2+} channels during cardiac action potential leads to Ca^{2+}-induced Ca^{2+} release from the sarcoplasmic reticulum (SR) [1–3]. These channels are subsequently inactivated by the elevation of the cytosolic Ca^{2+} concentration and by membrane depolarization [4,5]. Intracellular low pH is known to block the L-type Ca^{2+} channel and decrease the availability of the channels [6,7]. The property of L-type Ca^{2+} channel is important in regulation of the intracellular Ca^{2+} concentration and the action potential duration of cardiac myocytes.

Pathological conditions, such as valve disease, hypertension, or heart failure, may lead to hemodynamic or mechanical dysfunction of the heart, causing arrhythmia [8–12]. In these diseased hearts, myocytes are subjected to variable fluid pressure (FP) during contraction resulting from regurgitation, valve stenosis, and volume overload. Interestingly, in both whole heart preparations and *in situ* hearts, an increase in ventricular pressure shortens the duration of the action potential and the effective refractory period [8–11]. In addition, clinical evidence exists for a predisposition to fibrillation caused by regurgitant jets of blood in patients with valve incompetence [12], as well as for the occurrence of ectopic tachycardia in a patient with a catheter in the heart chamber [13]. In isolated rat ventricular myocytes, pressurized fluid flow (~16 dyn/cm^2), applied by micro-perfusion, suppresses the L-type Ca^{2+} current (I_{Ca}) [14,15]. The inhibition of the I_{Ca} by the FP, observed in single ventricular myocytes, could be one of the possible mechanisms that explain the shortenings of action potential and the effective refractory period during increases in ventricular pressure [8–11].

The main inhibitory mechanism in Ca^{2+} channels during FP in rat ventricular myocytes is an increase in intracellular Ca^{2+} transients [14]. Another inhibitory mechanism for the Ca^{2+} channel under FP involves intracellular acidosis resulting from activation of Cl^-–OH^- exchange [15]. It has been previously demonstrated that FP-induced intracellular acidosis is enhanced when myocytes are pretreated with a selective Na^+–H^+ exchange (NHE) inhibitor, HOE642 (cariporide: ((4-isopropyl-3-methylsulfonyl-benzoyl)-guanidine methane sulfonate) [16]. This suggests possible role for the activity of NHE in removing H^+ during FP stimulus. In the present study, we examined whether NHE plays a role in the regulation of the I_{Ca} during FP stimulus using the NHE inhibitor, HOE642, in rat ventricular myocytes under HEPES-buffered conditions. The

* Corresponding author. Address: College of Pharmacy, Chungnam National University, 220 Gung-dong, Yuseong-Gu, Daejeon 305-764, South Korea. Fax: +82 (0) 42 823 6566.
E-mail addresses: doctorkim@cnu.ac.kr (J.-C. Kim), shwoo@cnu.ac.kr (S.-H. Woo).

0006-291X/$ - see front matter © 2013 Elsevier Inc. All rights reserved.
http://dx.doi.org/10.1016/j.bbrc.2012.12.126

same micro-jet method previously described by Lee et al. [14] was used together with a whole-cell patch clamp technique. The present data indicate that NHE may reduce the suppressive effect of FP on the I_{Ca} by attenuating intracellular acidosis.

2. Materials and methods

2.1. Single cell isolation

Rat ventricular myocytes were enzymatically isolated from male Sprague–Dawley rats (200–300 g) using retrograde perfusion of the heart through the aorta (7 ml/min, at 36.5 °C) as described previously [14]. Rats were deeply anesthetized with sodium pentobarbital (150 mg/kg, *i.p.*), the chest cavity was opened and hearts were excised. This surgical procedure was carried out in accordance with university ethical guidelines.

2.2. Application of fluid pressure

Myocytes were continuously superfused with the Tyrode solution (in mM: 137 NaCl, 5.4 KCl, 10 HEPES, 1 $MgCl_2$, 10 glucose, 2 $CaCl_2$, pH 7.4). Pressurized flows of solutions were applied onto the single myocytes through a microbarrel (internal diameter = ~250 μm) as previously described [14,17]. The tip of microbarrel was placed at ≈150 μm from the cell and was connected to a fluid reservoir with 400-mm height. This height produced FP of about 16 dyn/cm^2 [14]. Electronic solenoid valve was installed in the middle of tubing connecting the fluid reservoir and the microbarrel, the tip of which, touching the chamber bottom, was tilted to one side with an angle of 45°. The positioning of the microbarrel was performed under microscope (TS2000, Nikon) using a micromanipulator (Prior England 48260).

The experimental cells were attached to the bottom of the chamber without a coating material. Using a microscope and video monitor, it was confirmed that no movement of the cell occurred during the fluid puffing before the start of the patch clamp experiments. The cells used for the recordings did not float or move at a FP of approximately 16 dyn/cm^2.

2.3. Current measurements and analysis

I_{Ca} was recorded using the whole-cell patch-clamp technique [18] using an EPC7 amplifier (HEKA, Germany). The patch pipettes were made of glass capillaries (Kimble Glass Inc.) to have resistance of 2–3 MΩ when filled with the internal solution containing (in mM) 110 CsCl, 20 TEA-Cl, 10 HEPES, 5 MgATP, and 2 EGTA, with the pH adjusted to 7.2 with CsOH; in some experiments 10 mM BAPTA was also included in the pipette solution (see Fig. 3). Outward K^+ currents were suppressed by replacing internal K^+ with Cs^+ and TEA^+, and inward rectifier K^+ current was suppressed by replacing external K^+ with Cs^+. Na^+ current was inactivated by holding the membrane potential at −40 mV. Trains of test pulses were to 0 mV for 120 ms with 0.1 Hz. The I_{Ca} was fully sensitive to 20 μM of nifedipine (data not shown) and to 200 μM Cd^{2+} [14]. Measurement of I_{Ca} was carried out 5–6 min after rupture of the membrane with the patch pipette, when the rundown of Ca^{2+} channels were slowed and stabilized. Generation of voltage protocols and acquisition of data were carried out using pCLAMP (9.0, Axon Instruments, CA, USA) combined with an A/D converter (Digidata 1322, Axon Instruments). The series resistance was 1.5–3 times the pipette resistance and was electronically compensated through the amplifier. The current signals were digitized at 10 kHz and low-pass filtered at 1 kHz.

We usually monitored raw currents as well as currents leak-subtracted by the P/N method ($N = 5$). Data in the figures are shown without leak subtraction to demonstrate that the cells had low, stable leak current. The % suppression of I_{Ca} by various interventions was evaluated after a gradual decrease in I_{Ca} by subtracting the rundown from the raw current [19]. Briefly, the time course of changes in peak I_{Ca} measured in the control conditions was fitted using double exponential curve fitting; the fitted curve was then considered to be a rundown component. The difference between the original time course and the fitted curve resulted in pure changes in I_{Ca}, which were used to measure percentage changes during the interventions.

Peak detection was performed with Clampfit (9.0, Axon Instruments), and the time constant (τ) of inactivation of I_{Ca} was obtained with single exponential curve fitting using the equation:

$$y = (A_i - A_f) \cdot \exp(-t/\tau) + A_f$$

where A_i and A_f are, respectively, the intitial ($t = 0$) and final (t = infinity) values of the parameter, and τ is a time constant of exponential decay.

HOE642 was dissolved in the external Tyrode solution and applied using the puffing apparatus or whole-chamber superfusion system depending on the experimental purposes. All the experiments were performed at room temperature (22–25 °C).

2.4. Statistics

Numerical results are presented as mean ± standard error of the mean (S.E.M.) (n = number of cells). A paired Student's t test was used to evaluate the statistical significance of differences between means. Differences at $P < 0.05$ were considered to be significant.

3. Results

3.1. Inhibition of Na^+–H^+ exchange suppresses I_{Ca} under fluid pressure

To examine whether NHE activity plays a role in the regulation of the I_{Ca} during FP stimulus, we used a specific NHE inhibitor, HOE642, in combination with FP exposure. In the whole-cell patch clamp mode, the application of FP of ~16 dyn/cm^2 suppressed the I_{Ca} by about 25% (compare '1' and '2' in Fig 1A; Fig 1B, $n = 7$, $P < 0.01$), which is consistent with a previous report on the effect of FP on the I_{Ca} [14]. When the inhibitory effect of FP on the I_{Ca} was stabilized, 10 μM HOE642 was applied in the continued presence of FP. Interestingly, HOE642 further suppressed the I_{Ca} (by about 40%, compared with the I_{Ca} recorded in the presence of FP only; compare '2' and '3' in Fig. 1A; $n = 7$, $P < 0.01$, Fig. 1B). The inhibitory effects of HOE642 under FP reached a maximum at 92.9 ± 6.44-s after the exposures ($n = 7$). Fig. 1C and D show that the inhibitory effect of HOE642 on the I_{Ca} under FP stimulus is dose-dependent. When the concentrations of HOE642 were gradually increased in the cells pre-exposed to FP (Fig. 1C), or in some cases single concentrations were used, the peak I_{Ca} was decreased by HOE642 in a dose-dependent manner (Fig. 1C, see representative currents, '3–5'), resulting in an IC_{50} of 0.97 ± 0.12 μM (Fig. 1D). Maximal inhibition by HOE642 was achieved at 100 μM, but there was only slight difference in the suppressive effects between 10 μM and 100 μM HOE642 (Fig. 1C and D). Fig. 1E and F compare current–voltage (I–V) relationships of the I_{Ca} recorded in the absence and presence of FP, and after the exposure to HOE642 (10 μM) in the presence of FP. The representative currents recorded at different test potentials show no voltage-dependence in the effects of HOE642 and FP on I_{Ca}, and no shift in the I–V curve in the presence of FP and HOE642 (Fig. 1F).

We next examined whether HOE642 shows a similar inhibitory effect on the I_{Ca} in the control myocytes (without FP). As shown in the Fig. 1G and H, application of HOE642 (10 μM) did not alter the

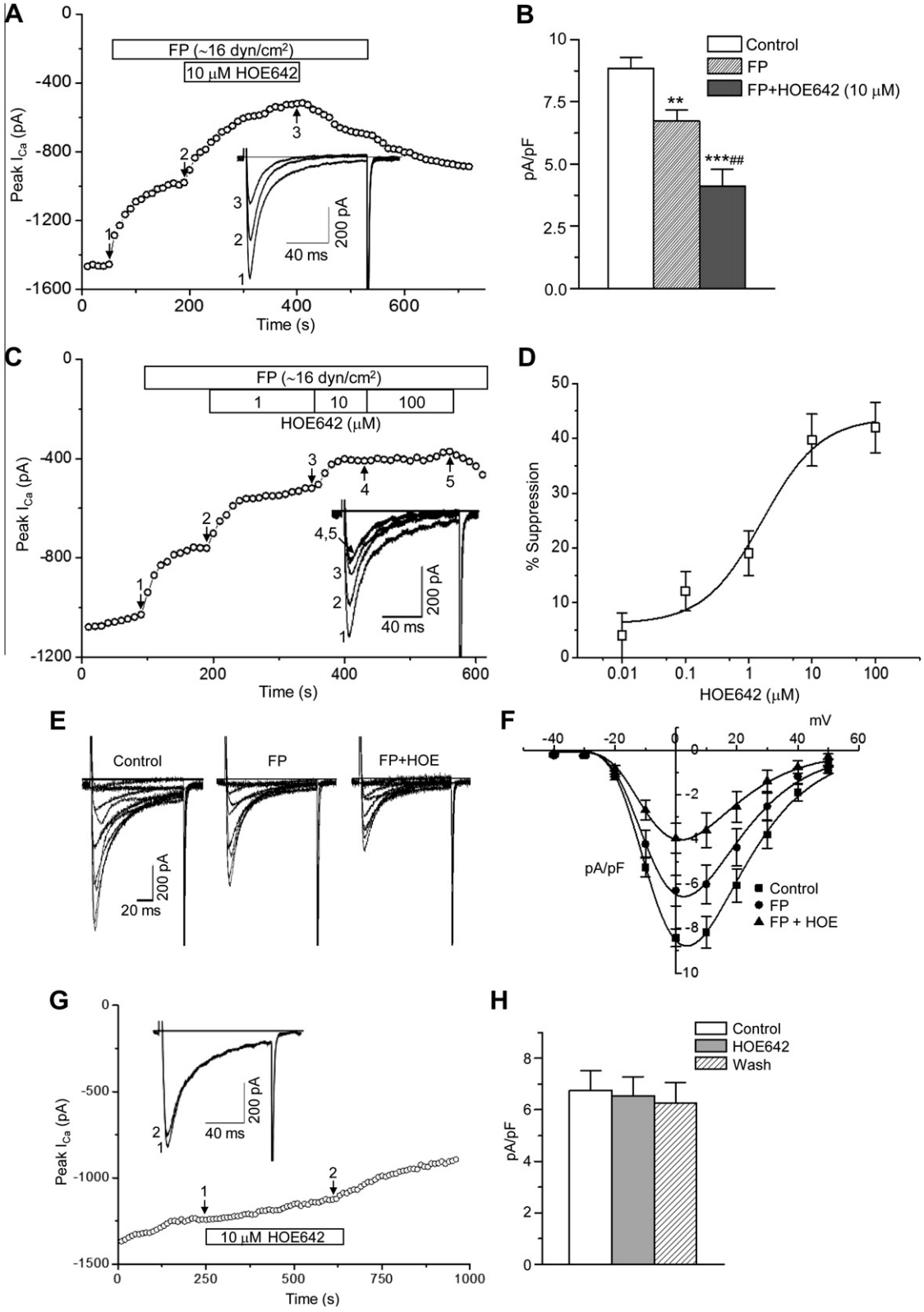

Fig. 1. Suppression of L-type Ca^{2+} current (I_{Ca}) by HOE642 in the myocytes pre-exposed to fluid pressure (FP). (A) Time course of the effects of FP (16 dyn/cm^2) and HOE642 (10 μM) on peak I_{Ca}. *Inset*, superimposed currents recorded at the numbered points. (B) Mean peak I_{Ca} (pA/pF) measured before and after the treatment of FP, and in HOE642 and FP. $^{**}P < 0.01$, $^{***}P < 0.001$ *vs.* Control. $^{\#\#}P < 0.01$ *vs.* FP ($n = 7$). (C) Time courses of the changes in peak I_{Ca} by FP and different concentrations of HOE642. *Inset* shows superimposed I_{Ca} recorded at the times marked by the numbers. (D) Concentration-dependent inhibition of I_{Ca} by HOE642 in the myocytes pre-exposed to FP (~16.3 dyn/cm^2). (E) Superimposed I_{Ca} recorded at different testing potentials ranging from −40 to +50 mV ($V_h = -40$ mV) in the control conditions (control), and after exposures to FP (~16.3 dyn/cm^2) and HOE642 (HOE, 10 μM). (F) Comparison of the mean current–voltage relationships of I_{Ca} measured under control condition, FP (~16.3 dyn/cm^2), and FP and HOE642 (HOE; 10 μM) ($n = 7$). (G) Time course of I_{Ca} change by HOE642 in control cells. (H) Mean peak I_{Ca} measured in the absence and presence of HOE642 (10 μM), and after the removal of HOE642 ($n = 7$).

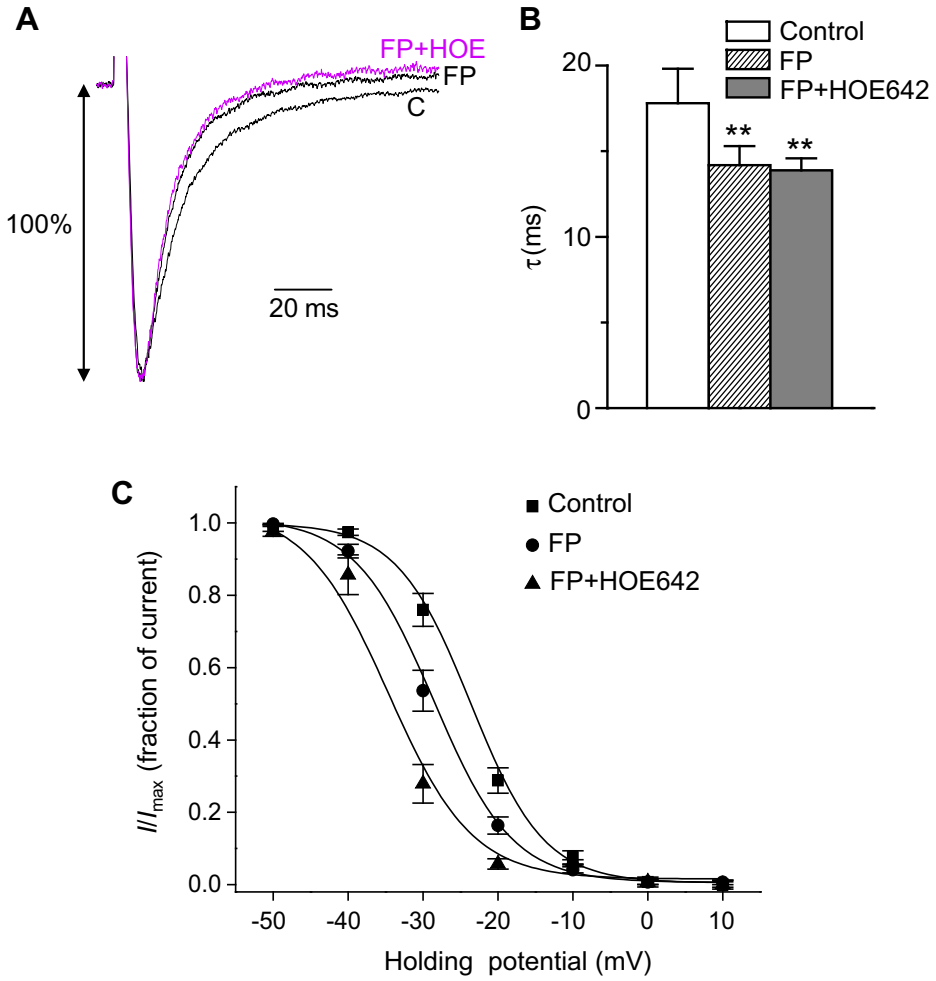

Fig. 2. No effect of HOE642 on the inactivation kinetics of I_{Ca} under FP. (A) Superimposed, peak-normalized I_{Ca}. (B) Mean inactivation time constants. $^{**}P < 0.01$ *vs.* Control ($n = 7$). (C) Averaged steady-state inactivation curves measured in the control conditions, after treatment of FP (16 dyn/cm^2) and FP plus HOE642 (10 μM) ($n = 6$). Measurements of steady state inactivation were carried out by applying prepossess to produce voltages ranging from −50 to +10 mV for 2.4 s from a V_h of −40 mV, followed by a test pulse to 0 mV for 100 ms. The peak amplitude of test pulse current was then plotted against the prepulse voltage. The individual peak currents were normalized to the peak I_{Ca} amplitude obtained at −50 mV.

I_{Ca} under control conditions (in pA/pF: control, 6.73 ± 0.75 *vs.* HOE642, 6.55 ± 0.74, $n = 7$, $P > 0.05$). We observed only a rundown of the peak I_{Ca}.

3.2. HOE642 causes a hyperpolarizing shift of steady-state inactivation of Ca^{2+} channels under FP

To examine whether the HOE642 exposure modulates the inactivation property of the Ca^{2+} channel, we evaluated the inactivation time constant (τ) of the I_{Ca} (see Section 2) in the absence of FP, and in the presence of FP with or without 10 μM HOE642. Fig. 2A shows the peak normalized, superimposed I_{Ca} traces recorded in each condition, indicating more rapid inactivation of the I_{Ca} under FP exposure, but no change in the inactivation time constant by HOE642. The decrease in the inactivation time constant by FP has been previously reported by Lee et al. [14]. Acceleration in the inactivation of the current is thought to be caused by enhanced Ca^{2+} release from the SR during depolarization [14]. In seven cells tested, the mean τ of I_{Ca} inactivation was 17.8 ± 2.01 ms in the control conditions, 14.2 ± 1.11 ms under FP exposure ($P < 0.01$ *vs.* control), and 13.9 ± 0.70 ms under HOE642 and FP exposures ($P > 0.05$ *vs.* FP), suggesting no effect of HOE642 on the inactivation kinetics of the I_{Ca} (Fig. 2B).

Fig. 2C illustrates the effect of HOE642 on the voltage-dependence of the availability of Ca^{2+} channels under FP exposure. Consistent with a previous report [14], the FP caused an approximately 4-mV left shift in the $V_{0.5}$ of the steady-state inactivation curve (see Section 2) without changing the slope factor. Additional treatment of 10 μM HOE642 in the presence of FP further shifted the steady-state inactivation curve in a hyperpolarizing direction ($\Delta V_{0.5}$: 6–7 mV) ('FP', −28.6 ± 1.2 mV *vs.* 'FP + HOE', −34.1 ± 0.9 mV, $n = 6$, $P < 0.001$).

3.3. Intracellular Ca^{2+} buffering does not alter the inhibitory effect of HOE642 under FP

FP has been reported to enhance Ca^{2+} transients evoked by depolarization in rat ventricular myocytes [14]. In addition, both ~80% of FP-induced I_{Ca} suppression and the acceleration of I_{Ca} inactivation in the presence of FP were found to be eliminated by intracellular high Ca^{2+} buffering [14]. We tested whether Ca^{2+} change during FP exposure plays a role in the suppressive effect of HOE642 on the I_{Ca} by introducing 10 mM BAPTA into the myocytes via a patch pipette. The effect of the FP on the I_{Ca} was greatly reduced in highly Ca^{2+}-buffered myocytes, but it still induced a small reduction in the I_{Ca} (about 4.5 ± 0.8% decrease, $n = 12$, $P < 0.05$ *vs.* control; Fig. 3A and B), which is consistent with the previous report [14]. However, the inhibitory effect of HOE642 (10 μM) on the I_{Ca} in the cells pre-exposed to FP was not significantly altered (by 42 ± 4.6% decrease, $n = 12$, $P < 0.001$ *vs.* FP; Fig. 3A and B; compare

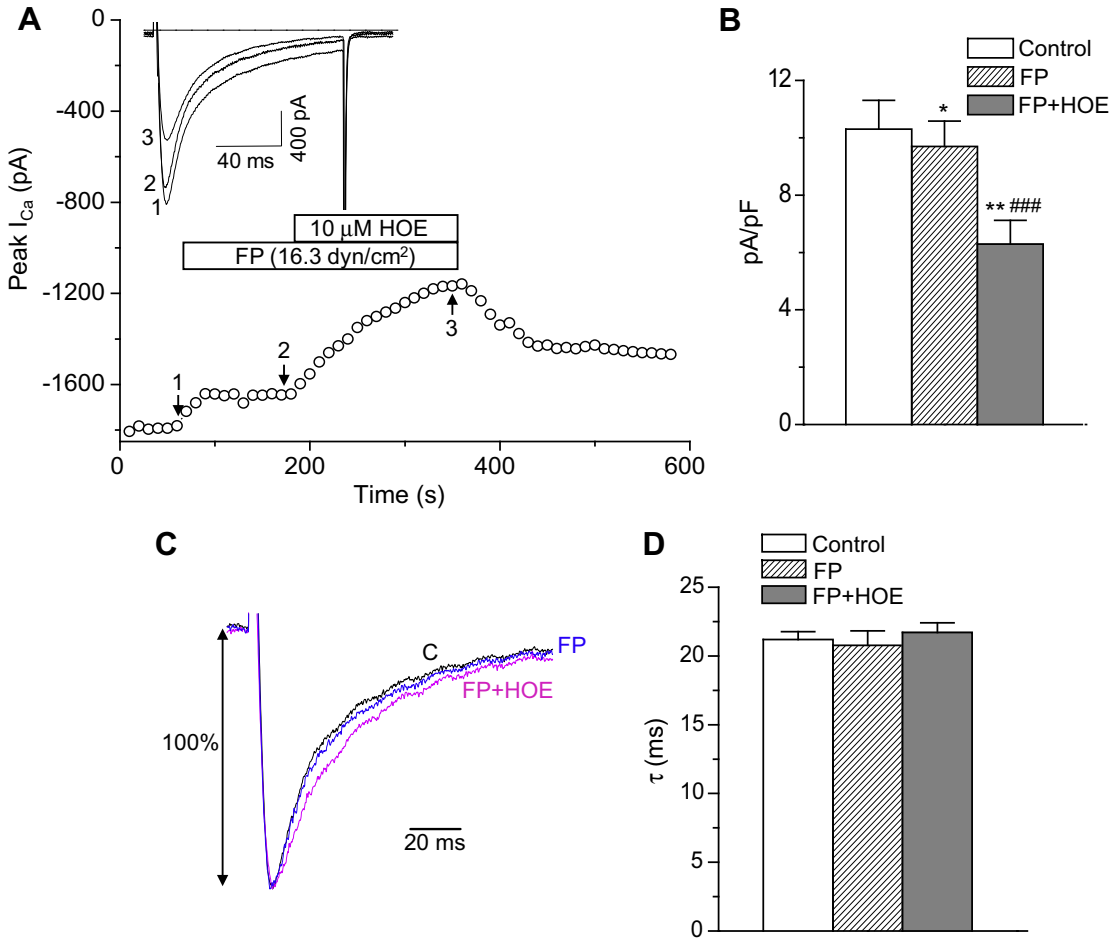

Fig. 3. Suppression of I_{Ca} by HOE642 in highly Ca^{2+}-buffered myocytes under FP. (A) Time course of the changes in I_{Ca} by FP and HOE642 (HOE) in a representative myocyte dialyzed with 10 mM BAPTA-containing solution. *Inset*, Superimposed currents recorded at the times indicated by the corresponding numbers. (B) Comparison of mean I_{Ca} among control, FP, and FP + HOE (10 μM; $n = 12$). $^{*}P < 0.05$, $^{**}P < 0.01$ *vs.* Control. $^{\#\#\#}P < 0.001$ *vs.* FP. (C) Peak-normalized current traces. (D) Mean inactivation time constants measured at control, FP, and FP + HOE ($n = 12$).

with Fig. 1B). As expected, high Ca^{2+} buffering removed the effect of FP on the inactivation of the I_{Ca} (see 'C' and 'FP' in Fig. 3C; Fig. 3D). Additional treatment with HOE642 yielded no further change in the inactivation kinetics (see 'FP' and 'FP + HOE' in Fig. 3C and D). This result indicates that the inhibition of I_{Ca} by HOE642 in the presence of FP may be independent of the increase in intracellular Ca^{2+}.

3.4. Blockade of HOE642-induced I_{Ca} suppression by removal of extracellular Cl^-

It has also been shown that intracellular acidosis inhibits I_{Ca} [6,7]. Application of FP not only enhanced Ca^{2+}-induced Ca^{2+} release during depolarization [14], but also induced intracellular acidosis [16]. A decrease in intracellular pH has been reported to be responsible for about 20% of the inhibition of I_{Ca} during FP exposure [15]. In addition, H^+-mediated I_{Ca} inhibition during FP stimulus was not affected by DIDS, a blocker of the Na^+–HCO_3^- exchange, but it was blocked by the removal of extracellular Cl^- [15]. These previous reports indicate that the Cl^--dependent acid loader may be responsible for the FP-induced I_{Ca} suppression via acidosis. We examined whether the suppressive effect of HOE642 on the I_{Ca} under FP is caused by an accumulation of H^+ by blocking the Cl^--dependent acid-loading mechanism. To block the Cl^--dependent acid loader, extracellular Cl^- was replaced by equimolar aspartate (final external $[Cl^-] = 0$ mM). When the Cl^- was replaced with the aspartate, the I_{Ca} was gradually decreased (data not shown). This effect was stabilized within 2–3 min after the treatment, consistent with previous reports [15,20]. Under these conditions, FP exposure inhibited the I_{Ca} by about 20% ($n = 6$, $P < 0.01$, 'low Cl^-_o' *vs.* 'low Cl^-_o + FP'; Fig. 4A and B). Interestingly, however, further application of HOE642 failed to have any effect on the I_{Ca} ($n = 6$, $P > 0.05$, 'low Cl^-_o + FP' *vs.* 'low Cl^-_o + FP + HOE642'; Fig. 4A and B). This result suggests that the inhibition of I_{Ca} by HOE642 in the presence of FP may be caused by H^+, accumulated by the Cl^--dependent acid loader (Cl^-–OH^- exchange in the current HEPES-buffered conditions [15,21]).

4. Discussion

In the present study, we showed that inhibition of NHE using HOE642 significantly reduces the I_{Ca} in rat ventricular myocytes under fluid pressure. In the cells exposed to FP, HOE642 induced a hyperpolarizing shift in the voltage-dependence of the steady-state inactivation curve without altering the inactivation kinetics of I_{Ca}. The effect of HOE642 on peak I_{Ca} was not affected by intracellular high Ca^{2+} buffering. However, it was completely inhibited by inhibition of the Cl^--dependent acid loading mechanism, which is known to be activated by FP, using zero extracellular Cl^- solutions. These results suggest that NHE may play an important role in balancing the H^+ concentration when ventricular myocytes are

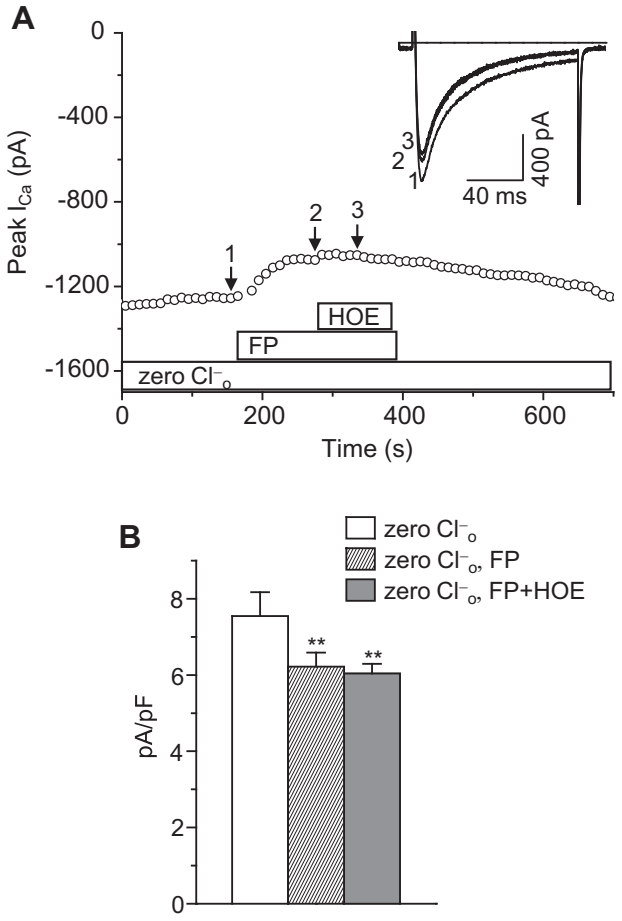

Fig. 4. Elimination of inhibitory effect of HOE642 on I_{Ca} by removal of extracellular Cl^-. (A) Time course of I_{Ca} change by FP and HOE642 (HOE) in cells pre-exposed to external zero Cl^- solutions. *Inset*: superimposed I_{Ca} recorded at the times marked by the corresponding numbers. (B) Mean peak I_{Ca} measured before (extracellular zero Cl^- solution) and after treatments of FP and FP + HOE642 in cells pre-exposed to the extracellular zero Cl^- solutions ($n = 6$). $^{**}P < 0.01$ *vs.* zero Cl^-_o.

exposed to FP, thereby attenuating the inhibitory effect of H^+ on L-type Ca^{2+} channels.

Inhibition of the suppressive effect of HOE642 on the I_{Ca} during FP exposure by the removal of external Cl^- suggests that NHE may be activated by intracellular acidosis caused by the Cl^--dependent acid loader during FP stimulus. The enhanced NHE activity due to the acidosis during the FP stimulus may result in increases in both the intracellular Na^+ concentration and the cell volume [22]. Possible volume increases through the activation of the regulatory volume increase process [23] may help cells recover from a shrinkage induced by FP (data not shown; [15]). In addition, the Na^+ accumulation may reduce the driving force of Na^+–Ca^{2+} exchange for removing Ca^{2+}, thereby increasing the intracellular Ca^{2+} concentration [24,25]. Most of the inhibitory effect of FP on I_{Ca} has been attributed to an increased intracellular Ca^{2+} concentration in rat ventricular myocytes [14]. When the inhibitory effect of FP on the I_{Ca} was stable, additional application of HOE642 decreased the I_{Ca} to a great extent (Fig. 1 A–C). This observation provides evidence that the inhibition of the I_{Ca} by FP via an increase in Ca^{2+} is not due to the Ca^{2+} loading via the NHE/Na^+–Ca^{2+} exchange-signaling hypothesis. In addition, intracellular high Ca^{2+} buffering largely inhibited the suppressive effect of FP on the I_{Ca}, but it did not alter the HOE642-induced reduction in the I_{Ca}. This finding also supports the idea that the inhibition of the I_{Ca} by HOE642 under FP exposure may not be related to a change in the intracellular Ca^{2+}.

The I_{Ca} underlies the action potential plateau and the refractory period of the action potential, and it triggers Ca^{2+} release from the SR [1–3]. The FP significantly decreases the I_{Ca} in ventricular myocytes. This reduces the duration of the action potential and the refractory period, thereby potentiating arrhythmias. Ventricular myocytes may be exposed to such FP and volume overload during valve diseases (e.g., aortic or pulmonary valve stenosis) and other hemodynamic disturbances. Under these conditions, the activity of NHE may prevent severe acidosis and thus attenuate the shortening of the action potential and ectopic beating by compromising H^+-induced I_{Ca} inhibition caused by fluid pressure. Due to the activity of NHE, the effect of the pH change on I_{Ca} during the FP exposure could be relatively small.

Paradoxically, the inhibitor of NHE, HOE642, has been suggested to be useful in preventing reperfusion damage of ischemic myocardium, which involves intracellular Ca^{2+} overload [26]. Blockade of cardiac type 1 NHE with HOE642 has been shown to protect cardiomyocytes against oxidant-induced cell death by preserving intracellular ion homeostasis and mitochondrial integrity [26]. During reperfusion of fluid after occlusion-induced ischemia, ventricular myocytes that are localized in the vicinity of the coronary artery may be exposed to instant high hydrostatic pressure. Under this condition, the I_{Ca} may be inhibited by the FP, and HOE642 treatment may also further decrease the I_{Ca}. This may help cells prevent Ca^{2+} overloading and Ca^{2+}-overload-induced arrhythmias. Our data may provide a possible mechanism for the cardioprotective effect of HOE642 in ischemia–reperfusion damage of ventricular myocytes.

Acknowledgments

We thank to Sanofi-Aventis (Deutschland GmbH, Germany) for kindly providing us HOE642.

This work was supported by the National Research Foundation of Korea (NRF) grants funded by the Korea Government (MEST) (2011-0015637, 2011-0006681).

References

[1] A. Fabiato, Calcium-induced release of calcium from the cardiac sarcoplasmic reticulum, Am. J. Physiol. 245 (1983) 1–14.
[2] D.J. Beuckelmann, W.G. Wier, Mechanism of release of calcium from sarcoplasmic reticulum of guinea-pig cardiac cell, J. Physiol. 405 (1988) 233–255.
[3] M. Näbauer, G. Callewaert, L. Cleemann, M. Morad, Regulation of calcium release is gated by calcium current, not gating charge, in cardiac myocytes, Science 244 (1989) 800–803.
[4] R.S. Kass, M.C. Sanguinetti, Inactivation of calcium channel current in the calf cardiac Purkinje fiber, evidence for voltage- and calcium-mediated mechanisms, J. Gen. Physiol. 84 (1984) 705–726.
[5] K.S. Lee, E. Marban, R.W. Tsien, Inactivation of calcium channels in mammalian heart cells: joint dependence on membrane potential and intracellular calcium, J. Physiol. 364 (1985) 395–411.
[6] S. Vogel, N. Sperelakis, Blockade of myocardial slow inward current at low pH, Am. J. Physiol. 233 (1977) C99–C103.
[7] Y. Kurachi, The effects of intracellular protons on electrical activity of single ventricular cells, Pflügers Arch. 394 (1982) 264–270.
[8] M.J. Lab, Mechanoelectric feedback (transduction) in heart: concepts and implications, Cardiovasc. Res. 32 (1996) 3–14.
[9] B.B. Lerman, D. Burkhoff, D.T. Yue, M.R. Franz, K. Sagawa, Mechanoelectric feedback: independent role of preload and contractility in modulation of canine ventricular excitability, J. Clin. Invest. 76 (1985) 1843–1850.
[10] J.H. Levine, T. Guarnieri, A.H. Kadish, R.I. White, H. Calkins, J.S. Kan, Changes in myocardial repolarization in patients undergoing balloon valvuloplasty for congenital pulmonary stenosis: evidence for contraction-excitation feedback in humans, Circulation 77 (1988) 70–77.
[11] M.R. Franz, D. Burkhoff, D.T. Yue, K. Sagawa, Mechanically induced action potential changes and arrhythmia in isolated and *in situ* canine hearts, Cardiovasc. Res. 23 (1989) 213–223.
[12] S.A. Nazir, M.J. Lab, Mechanoelectric feedback and atrial arrhythmias, Cardiovasc. Res. 32 (1996) 52–61.
[13] J. Conwell, M. Cocalis, L. Erickson, EAT to the beat: 'ectopic' atrial tachycardia caused by catheter whip, Lancet 342 (1993) 740.

[14] S. Lee, J.C. Kim, Y. Li, M.J. Son, S.H. Woo, Fluid pressure modulates L-type Ca^{2+} channel via enhancement of Ca^{2+}-induced Ca^{2+} release in rat ventricular myocytes, Am. J. Physiol. Cell Physiol. 294 (2008) C966–C976.
[15] J.C. Kim, M.J. Son, S.H. Woo, Suppression of L-type Ca^{2+} current by fluid pressure in rat ventricular myocytes: possible role of Cl^{-}–OH^{-} exchange, Biochem. Biophys. Res. Commun. 413 (2011) 17–23.
[16] J.C. Kim, S.H. Woo, Decrease of intracellular pH and activation of Na^{+}–H^{+} exchanger by fluid pressure in rat ventricular myocytes, Yakhak Hoechi 55 (3) (2011) 247–250.
[17] S.H. Woo, T. Risius, M. Morad, Modulation of local Ca^{2+} release sites by rapid fluid puffing in rat atrial myocytes, Cell Calcium 41 (2007) 397–403.
[18] O.P. Hamill, A. Marty, E. Neher, B. Sakmann, F.J. Sigworth, Improved patch-clamp techniques for high-resolution current recording from cells and cell-free membrane patches, Pflügers Arch. 319 (1981) 85–100.
[19] R. Marrannes, E. De Prins, Computer programs to facilitate the estimation of time-dependent drug effects on ion channels, Comput. Methods Programs Biomed. 74 (2004) 167–181.
[20] S.S. Zhou, G. Zhan, L. Dong, Y.F. Ding, X.D. Zhang, Y.M. Wang, J.M. Pei, F. Gao, X.L. Ma, Anion channels influence ECC by modulating L-type Ca^{2+} channel in ventricular myocytes, J. Appl. Physiol. 93 (2002) 1660–1668.
[21] B. Sun, C.H. Leem, R.D. Vaughan-Jones, Novel chloride-dependent acid loader in the guinea-pig ventricular myocytes: part of a dual acid-loading mechanism, J. Physiol. 495 (1996) 65–82.
[22] M. Karmazyn, X.T. Gan, R.A. Humphreys, H. Yoshida, K. Kusumoto, The myocardial Na^{+}–H^{+} exchange. Structure, regulation, and its role in heart disease, Circ. Res. 85 (1999) 777–786.
[23] S.F. Pedersen, M.E. O'Donnell, S.E. Anderson, P.M. Cala, Physiology and pathophysiology of Na^{+}/H^{+} exchange and Na^{+}–K^{+}–$2Cl^{-}$ cotransport in the heart, brain, and blood, Am. J. Physiol. Regul. Integr. Comp. Physiol. 291 (2006) R1–R25.
[24] F.F.T. Ch'en, R.D. Vaughan-Jones, K. Clarke, D. Noble, Modelling myocardial ischemia and reperfusion, Prog. Biophys. Mol. Biol. 69 (1998) 515–538.
[25] B.V. Alvarez, N.G. Pérez, I.L. Ennis, M.C. Camilion de Hurtado, H.E. Cingolani, Mechanisms underlying the increase in force and Ca^{2+} transient that follow stretch of cardiac muscle: a possible explanation of the Anrep effect, Circ. Res. 85 (1999) 716–722.
[26] Y. Teshima, A. Masaharu, S.P. Jones, E. Marban, Cariporide (HOE642), a selective Na^{+}–H^{+} exchange inhibitor, inhibits the mitochondrial death pathway, Circ. Res. 108 (2003) 2275–2281.